Self-Heating Measurements for a Dual-Phase Steel under Ultrasonic Fatigue Loading for stress amplitudes below the conventional fatigue limit

Noushin Torabian[a,b,*], Véronique Favier[a], Saeed Ziaei-Rad[b],
Frédéric Adamski[a], Justin Dirrenberger[a], Nicolas Ranc[a]

[a]Laboratoire PIMM, UMR CNRS 8006, Arts et Métiers Paris Tech, Paris 75013, France
[b]Department of Mechanical Engineering, Isfahan University of Technology, Isfahan 84156-83111, Iran

Abstract

The aim of the present research was to study the self-heating behavior of a dual-phase steel under ultrasonic fatigue loading for stress amplitudes lower than the conventional fatigue limit. The steel studied in this research was DP600 commercial dual phase steel. Fatigue tests were conducted for different values of stress amplitudes up to 10^7 cycles using an ultrasonic fatigue machine at a testing frequency of 20 kHz with flat specimens. An infrared camera was used to measure the mean temperature evolution during the tests. A specific form of heat diffusion equation was adopted in this work to calculate the intrinsic dissipation from temperature measurements. The variation of the dissipated energy versus stress amplitude under cyclic loading was also studied.
© 2016 The Authors. Published by Elsevier B.V.

1. Introduction

Since the first conference in Paris in 1998, the fatigue behavior of metallic materials in the very high cycle fatigue (VHCF) regime ($N_f \geqslant 10^7$) has been investigated by various research groups (Miller et al. 1999). Ultrasonic fatigue testing is an effective tool to carry out VHCF tests. Due to the extremely high loading frequency of 20 kHz,

ultrasonic fatigue machine considerably reduces the testing time and makes it possible to investigate the VHCF properties of different high strength steels in a reasonable time (Wu et al., 1994, Stanzl-Tschegg et al., 1993). For instance, it takes 14 hours to reach 10^9 cycles with ultrasonic loading, while using the conventional fatigue machines with a working frequency of 100 Hz, a time period of 4 months is required to go up to 10^9 cycles. About the application of the ultrasonic testing frequency, most researchers believe that frequency effect itself is small in most cases at low stress amplitudes and does not change the essence of fatigue (Wang et al. 1999, Furuya et al. 2002, Marines et al. 2003). However, the thermal effect induced by loading with ultrasonic frequency is still questionable. The aim of the present work is to conduct a thermography study on a dual-phase steel under ultrasonic fatigue loading at low stress amplitudes.

Dual-phase (DP) steels are a group of advanced high strength steels which contain hard martensite islands dispersed in soft ferrite matrix. Due to the characteristics of high strength, good ductility, low yielding to tensile ratio, and high initial work hardening rates, DP steel has a broad application in automotive industries.

In several research works the dissipated energy was deduced from self-heating measurements in the case of dual-phase steels during low frequency fatigue loadings (Boulanger et al. 2004, Munier et al. 2010, Doudard et al. 2009, Doudard et al. 2010). Concerning ultrasonic fatigue testing (20 kHz), Blanche et al. (2015) as well as Ranc et al. (2015) developed methods to identify dissipative fields from IR thermography measurements for pure copper .

The present paper aims at studying the thermal response of DP600 commercial dual-phase steel under ultrasonic fatigue loading for stress amplitudes lower than the conventional fatigue limit. Successive fatigue tests with increasing the stress amplitude were carried out by means of ultrasonic fatigue machine with the working frequency of 20 kHz. Infrared thermography was employed to record the mean temperature on the surface of the specimen. Self-heating diagrams were developed for this material based on mean temperature. The mean dissipated energy per cycle was estimated as a function of the stress amplitude.

2. Material and experimental procedure

2.1. Material characterization

The material used in this study is DP600 dual-phase steel with chemical composition of 0.933%Mn, 0.040%P, 0.213%Si, 0.727%Cr, 0.075%C, 0.039%Al, and 0.042%Nb (Munier et al, 2010). This commercial ferritic-martensitic dual-phase steel contains 15wt% of martensite and was received as sheets of 3 mm thickness. It was supplied by AreclorMittal Company. Fig. 1 shows the microstructure of the material obtained from SEM observations. The mechanical properties of DP600 in the transverse direction are presented in Table 1.

Table 1. Mechanical properties of DP600 steel (Munier et al. 2010).

Young's Modulus, GPa	Yield strength, MPa	Ultimate tensile strength, MPa	Elongation, %
210	420	610	20

2.2. Ultrasonic fatigue loadings

Fatigue tests were conducted using an ultrasonic fatigue machine at a testing frequency of 20 kHz with flat specimens. The specimen dimensions were calculated so that the free resonant frequency of the specimen in the first longitudinal mode is 20 kHz. The specimens were machined in the transverse direction. All specimens were mechanically and then electrolytically polished to remove all hardened layers on the specimen surface and consequently release the residual stresses. Fig. 2 illustrates the geometry of the fatigue specimens.

During the tests, an infrared camera (320×256 pixels) was used to monitor the temperature field on the specimen surface. The specimen surface was painted in matte black to have a uniform surface emissivity close to 1. From the temperature measurements, the intrinsic dissipation was determined using a heat diffusion model as explained in the following section. Fig. 3 shows the ultrasonic equipment and the camera. Successive steps of fatigue tests were conducted by increasing the stress amplitude. The tests were limited to low stress amplitudes i.e. the stress values lower than the conventional fatigue limit which equals to 250 MPa according to Munier et al. (2010).
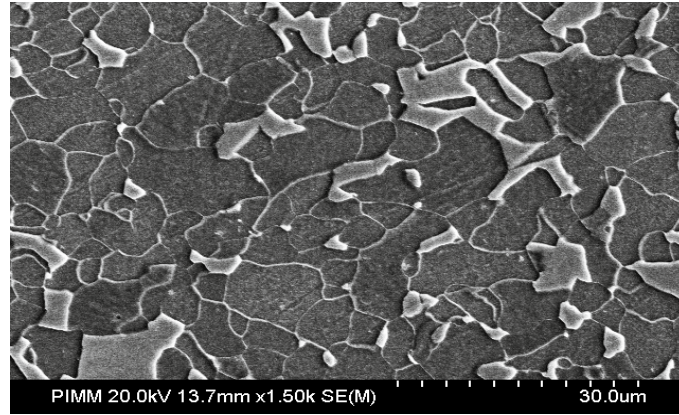
Fig. 1. SEM micrograph of the DP600 sample, (bright grains are martensite and dark grains are ferrite).

Therefore, series of fatigue loadings were carried out by increasing the stress amplitude from 57 MPa to 241 MPa. At each stress amplitude the fatigue test was carried out up to 10^7 cycles and the mean temperature evolutions were registered during the tests. At the end of each step the testing machine was stopped and temperature measurements were continued for 2 minutes to record the natural cooling of the specimen after unloading. Between two following steps there was a time gap of around 10 minutes to restart at equilibrium. In all cases, the temperature was measured at the center of the gauge part of the specimen.

2.3. Determination of the dissipated energy

As proposed by Boulanger et al. (2004), by assuming the material parameters such as the specific heat and the conduction coefficient to be constant and by introducing the temperature increase $\theta = T - T_0$, the heat diffusion equation can be written as:

$$\rho C \dot{\theta} + \rho C \frac{\theta}{\tau} = s_{the} + d_1 \tag{1}$$

where ρ is the mass density, C is the specific heat, s_{the} is the thermoelastic source, and d_1 is the intrinsic heat dissipation. For the DP600 steel $\rho = 7800 kg/m^3$ and $C = 460 J/kg/°C$ (Chrysochoos et al. 2008). τ is a time constant describing the thermal exchanges between the specimen and its environment.
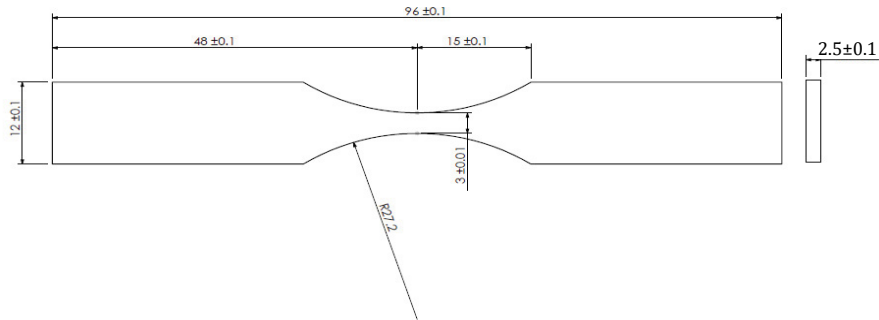

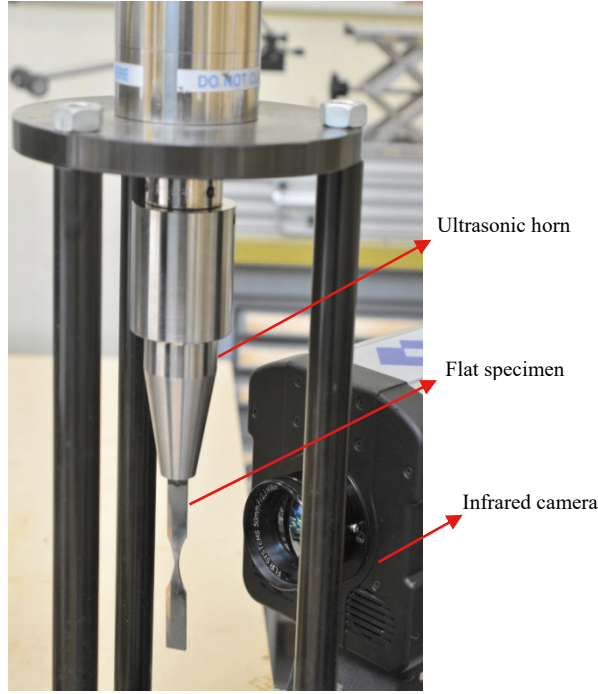Fig. 2.   Fatigue test specimen geometry (all dimensions are in mm).

Fig. 3   Ultrasonic fatigue testing equipment.

The time constant τ can be determined at the end of the test, just after the unloading when there is no applied stress; at this moment the thermoelastic and intrinsic dissipation heat sources are zero while the temperature change is not null ($\theta \neq 0$). Therefore the heat equation is reduced to:

$$\rho C \dot{\theta} + \rho C \frac{\theta}{\tau} = 0 \tag{2}$$

Solving the above equation, the theoretical relation for temperature change is obtained as:

$$\theta(t) = \theta_f \exp(\frac{-t}{\tau}) \tag{3}$$

where θ_f is the temperature increase measured when the loading stops. Thus τ is estimated by fitting the experimental data with the theoretical evolution of θ. Moreover, since the loading frequency is high, because of the temporal inertia, it is not possible to measure the instantaneous value of θ but only its average value determined over numerous loading cycles, therefore by denoting:

$$\tilde{u} = \frac{1}{nT_1} \int_t^{t+nT_1} u \, dt = \frac{f}{n} \int_t^{t+T_1} u \, dt \tag{4}$$

where T_1 is the period of the loading, f is the loading frequency and n is the number of cycles. The heat diffusion equation after the integration explained above is re-written as:

$$\rho C \dot{\tilde{\theta}} + \rho C \frac{\tilde{\theta}}{\tau} = \tilde{s}_{the} + \tilde{d}_1 \tag{5}$$

As stated by Boulanger et al. (2004), the sum of the thermoelastic power over one loading cycle is null ($\tilde{s}_{the} = 0$). Therefore, in the stabilized regime, when $\dot{\tilde{\theta}}=0$, the average intrinsic dissipation determined over numerous loading cycles is easily determined from Eq. (5) as:

$$\rho C \frac{\tilde{\theta}}{\tau} = \tilde{d}_1 \qquad (6)$$

The mean dissipated energy per cycle can be obtained as $\tilde{d}_1/f$, where f is the loading frequency.

3. Results

Fig. 4 shows the evolution of the temperature for some of the loading steps. This figure shows that for each loading step, the temperature increased suddenly in the early stages of loading (after around 10^6 cycles) and then gradually reached a steady state. In fact the stabilization of the temperature corresponded to a balance between the mechanical energy dissipated into heat and the energy lost by convection and radiation at the specimen surface and by conduction inside the specimen. The higher the stress amplitude, the higher was the rate of temperature increase. The mean steady state temperature elevation for each loading step defined as $\theta_f = T_{steady} - T_{initial}$ is plotted versus stress amplitude in Fig. 5. From this figure it is clear that by increasing the stress amplitude, the temperature elevation increased; for stress amplitudes lower than 60 MPa the temperature increase remains lower than 10°C, however it reaches around 70°C for higher stress amplitudes.
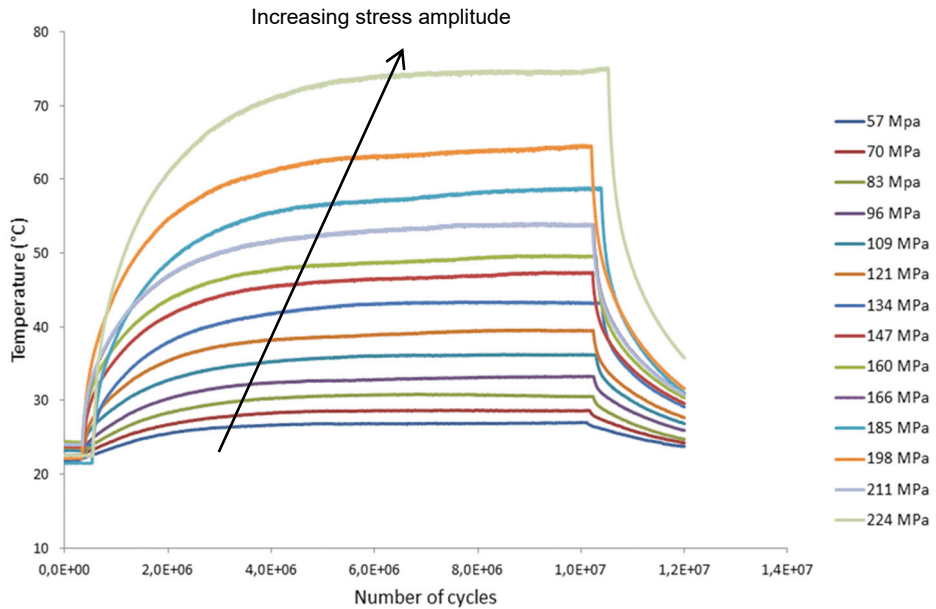

Fig. 4   Evolution of the mean temperature during several series of ultrasonic cyclic loadings (R=-1, f =20kHz).
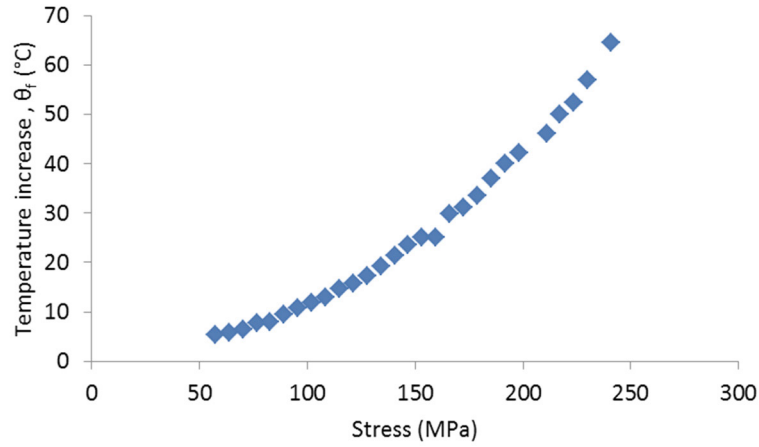
Fig. 5   Temperature increase versus stress amplitude for the DP600 steel under ultrasonic fatigue loading.

Fig. 6 shows the values of the time constant τ obtained by matching Equation (3) and the experimental evolution curve of temperature with time after the stop of the fatigue test for various stress amplitudes. By increasing the stress amplitude up to 127 MPa, τ decreased from around 20 s to 8 s, however after this point it reached a plateau and remained approximately constant by increasing the stress. Taking into account the value of τ for the different stress amplitudes, the mean dissipated energy per cycle was calculated from the steady state temperature. Fig. 7 depicts the change in dissipated energy per cycle as a function of stress amplitude. From this figure it is clear that the higher the stress amplitude, the higher was the dissipated energy. Moreover the dissipated energy per cycle is a quadratic function of stress amplitude.
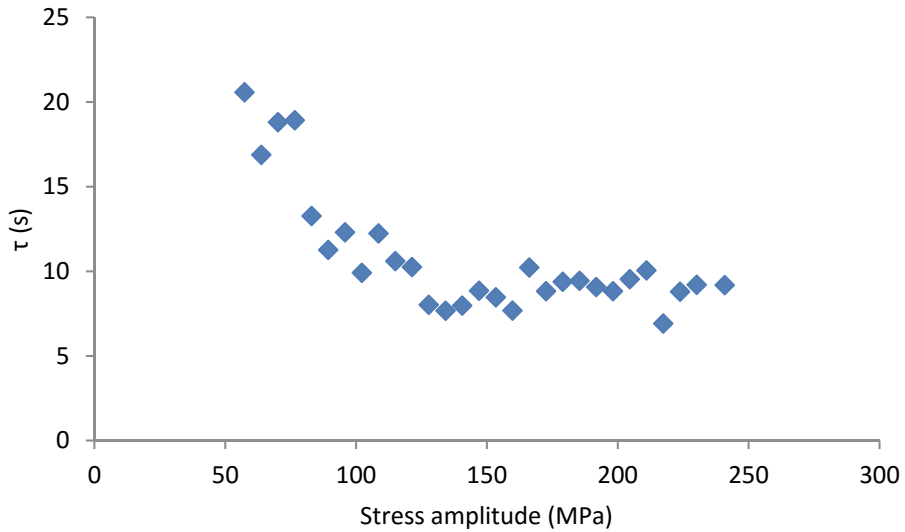

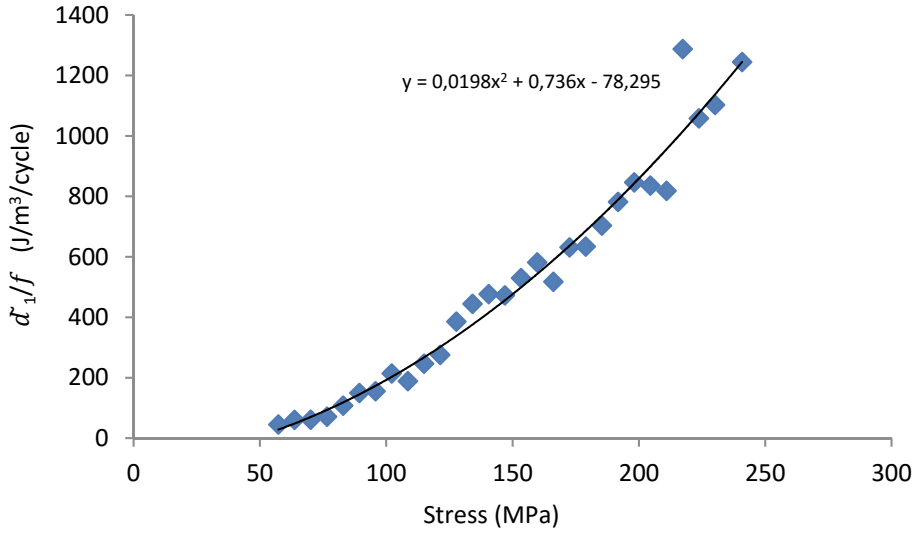Fig.6   The time constant, τ, versus stress amplitude.

Fig. 7 Mean dissipated energy per cycle versus stress amplitude, for the DP600 steel under ultrasonic loading.

4. Discussion

For low stress amplitudes, below 250 MPa, the change in dissipated energy per cycle versus stress amplitude displayed a quadratic form and so a gradual increase in the slope of the curve was observed. In contrast, as reported in the literature, low frequency cyclic loadings revealed a strong change in the slope of these curves from a particular stress amplitude. The latter was related to endurance limit (Munier et al. 2010, Luong 1998, La Rosa and risitano 2000) or to a change in dissipative mechanisms (Mareau et al. 2009). Considering that the dissipated energy is due to a viscoelastic or viscous material behavior characterized by constant properties leads to the following expressions for the dissipated energy (Mareau et al. 2009); assuming a prescribed sinusoidal stress with the amplitude σ_a and a Kelvin-Voigt model (spring and dashpot in parallel), the dissipated energy per cycle is written as:

$$\frac{\tilde{d}_1}{f} = \frac{1}{f} \frac{2\eta(\pi\sigma_a)^2}{\frac{\mu^2}{f^2} + 4\pi^2\eta^2} \tag{7}$$

where μ and η are the elastic and viscous moduli, respectively.

In the case of a pure viscous behavior and a zero mean stress, the dissipated energy per cycle is written as (Mareau et al. 2009):

$$\frac{\tilde{d}_1}{f} = \frac{1}{f} \frac{\sigma_a^2}{2\eta} \tag{8}$$

In both cases, in the case of constant material properties (μ and η), the dissipated energy per cycle is a quadratic function of the stress amplitude. In this work, as the dissipated energy per cycle was found to be a quadratic function of the stress amplitude for low stress amplitudes, it can be assumed that the material internal state remains nearly the same during cyclic loading. As the hardness of the martensite is much higher than ferrite, dislocations are assumed to move only in the ferritic phase. Because of the high frequencies and as discussed by Favier et al. (2016) for α-

iron, the "low-temperature" behavior, typical of body-centered cubic structure, prevailed at room temperature for 20 kHz cyclic loading. As a result, the dissipated energy was probably due to the to-and-fro motion of edge dislocations. This motion occurred in a non-hardening quasi reversible manner leading to very slight changes in the microstructure.

5. Conclusions

In this work, ultrasonic fatigue tests along with in-situ infrared thermography were conducted on flat specimens of DP600 dual-phase steel. The self-heating diagrams were developed under ultrasonic loading for low stress amplitudes and the dissipated energy per cycle was also determined. It was observed that at low stress amplitudes the dissipated energy per cycle is a quadratic function of the stress amplitude. This behavior under ultrasonic loading is different form the results reported in the literature under low frequency fatigue tests, for which there is a sudden change in the slope of the dissipation-stress diagram as a result of the change in heating mechanism. Moreover, the internal friction which stems from dislocation motions can be considered as the main dissipative mechanism for this case.

References

Blanche, A., Chrysochoos, A., Ranc, N., Favier, V., 2015. Dissipation assessments during dynamic very high cycle fatigue tests. Experimental Mechanics 55, 699–709.

Boulanger, T., Chrysochoos, A., Mabruand C., Galtier, A., 2004. Calorimetric analysis of dissipative and thermoelastic effects associated with the fatigue behavior of steels. International Journal of Fatigue 26, 221–229.

Chrysochoos, A., Berthel, B., Latourte, F., Pagano, S., Wattrisse, B., Weber, B ., 2008. Local energy approach to steel fatigue. Strain 44, 327–334.

Doudard, C., and Calloch, S., 2009. Influence of hardening type on self-heating of metallic materials under cyclic loadings at low amplitude. European Journal of Mechanics-A/Solids 28, 233–240.

Doudard, C., Calloch, S., Hild, F., Roux, S., 2010. Identification of heat source fields from infrared thermography: Determination of 'self-heating' in a dual-phase steel by using a dog bone sample. Mechanics of Materials 42, 55–62.

Favier, V., Blanche, A., Wang, C., Phung, N. L., Ranc, N., Wagner, D., Bathias, C., Chrysochoos A., Mughrabi, H., 2016. Very High Cycle Fatigue for single phase ductile materials: comparison between alpha-iron, copper and alpha-brass polycrystals. International Journal of Fatigue, submitted.

Furuya, Y., Matsuoka, S., Abe, T., Yamaguchi, K., 2002.Gigacycle fatigue properties for high-strength low-alloy steel at 100 Hz, 600 Hz, and 20 kHz. Scripta Materialia 46, 157–62.

La Rosa G., Risitano A., 2000. Thermographic methodology for rapid determination of the fatigue limit of materials and mechanical components. International Journal of Fatigue 22, 65–73.

Luong, M., 1998. Fatigue limit evaluation of metals using an infrared thermographic technique. Mechanics of Materials 28, 155–163.

Mareau, C., Favier, V., Weber, B., Galtier, A., 2009. Influence of the free surface and the mean stress on the heat dissipation in steels under cyclic loading. International Journal of Fatigue 31, 1407–1412.

Marines I., Dominguez, G., Baudry, G., Vittori, J.F., Rathery, S., Doucet, J.P., 2003. Ultrasonic fatigue tests on bearing steel AISI-SAE 52100 at frequency of 20 and 30 kHz. International Journal of Fatigue 25, 1037–1046.

Miller, K.J., Bathias, C., Stanzl-Tschegg, S.E., 1999. Gigacyle Fatigue. Fatigue and Fracture of Engineering Materials and Structures 22, 545–728.

Munier. R., Doudard, C., Calloch, S., Weberb, B., 2010. Towards a faster determination of high cycle fatigue properties taking into account the influence of a plastic pre-strain from self-heating measurements. Procedia Engineering 2, 1741–1750.

Ranc, N., Blanche, A., Ryckelynck, D., Chrysochoos, A., 2015. POD preprocessing of IR thermal data to assess heat source distributions. Experimental Mechanics 55, 725–739.

Stanzl-Tschegg, S.E., Mayer, H.R., Tschegg, E.K., 1993. High frequency method for torsion fatigue testing. Ultrasonics 31, 275–280.

Wang, Q.Y., Berard, J.Y., Dubarre, A., Baudry, G., Rathery, S., Bathias, C., 1999. Gigacycle fatigue of ferrous alloys. Fatigue and Fracture of Engineering Materials and Structures 22, 667–72.

Wu, T., Bathias, C., 1994. Application of fracture mechanics concept to ultrasonic fatigue. Engineering Fracture Mechanics 47, 683–690.